Synthesis, Ligand Binding and Biomimetic Oxidations of Deuterohaemin modified with an Undecapeptide Residue

Luigi Casella,*[a] Michele Gullotti,[a] Luca De Gioia,[a] Enrico Monzani[a] and Francesco Chillemi[b]

[a] *Dipartimento di Chimica Inorganica e Metallorganica, Centro C.N.R., Università di Milano, Via Venezian 21, 20133 Milano, Italy*

[b] *Dipartimento di Chimica Organica e Industriale, Università di Milano, Via Golgi 19, 20133 Milano, Italy*

Deuterohaemin [(3,7,12,17-tetramethylporphyrin-2,18-dipropionato)iron(III)] has been covalently linked to the undecapeptide Ala-Phe-Ser-Phe-Glu-Ala-Gln-Gly-Gly-Leu-Ala at one of the propionic acid side chains. The binding equilibria between the resulting deuterohaemin–undecapeptide complex and imidazole occur in two steps; the first molecule of the ligand binds with high affinity (K_1 = 1500 dm^3 mol^{-1}), while for the second molecule the affinity is markedly lower (K_2 = 220 dm^3 mol^{-1}), indicating that folding of the peptide chain in the monoimidazole adduct severely limits the accessibility of the sixth iron co-ordination position. The complex exhibits both catalase and peroxidase activity towards reducing substrates in the presence of hydrogen peroxide. In catalytic sulphoxidations of a series of *para*-substituted thioanisoles, *p*-XC_6H_4SMe, by hydrogen peroxide a good correlation has been found between the relative rates and the Hammett σ_p values, indicating that direct oxygen transfer from the active oxoiron species to the sulphide is probably operative. The kinetics of the catalytic oxidation of tyrosine by hydrogen peroxide in the presence of the complex, producing the oxidative coupling dimer *o*,*o*′-dityrosine, was also studied. It is consistent with a mechanism involving the initial binding of the phenolic substrate to the active catalyst to form an intermediate complex, and its subsequent breakdown in the rate-determining step of the catalytic cycle. The results obtained in the biomimetic oxidations are compared with those of the corresponding peroxidase-catalysed reactions.

There is increasing interest in the synthesis of polypeptide-bound metalloporphyrins as models for haem-containing oxygenase and peroxidase enzymes.[1–8] These haem model systems are obtained by covalent linking of peptide residues to the side chains of the porphyrins or proteolytic degradation of natural haemoproteins, but there are also reports on the inclusion of simple metalloporphyrins in polypeptide or protein matrices such as serum albumin.[9] The main scope of introducing such peptide chains is to provide an environment to the haem that mimics to some extent that present in the enzymes. In this respect, the peptide-containing haems represent an emerging class of artificial enzymes which should improve the simple metalloporphyrin complexes currently used as biomimetic catalysts for oxidation and oxygenation processes.[10–12]

As the first attempt in the development of synthetic routes to new families of peptide-bound haemin complexes we report here the preparation, characterization and catalytic activity of the deuterohaemin–undecapeptide complex **1**. The undecapeptide used in the synthesis of **1** has been reported recently.[13] It corresponds to amino acid sequence 51–61 of α-chain DP from human histocompatibility class II membrane glycoprotein, an antigen expressed by B lymphocytes; it was used here for its moderate size and because the presence of polar and acidic groups in the amino acid side chains ensures sufficient solubility in a protic medium in the presence of relatively small amounts of bases. Deuterohaemin [(3,7,12,17-tetramethylporphyrin-2,18-dipropionato)iron(III)] was preferred to the more common protohaemin[(3,7,12,17-tetramethyl-8,13-divinylporphyrin-2,18-dipropionato)iron(III)] because it does not contain the oxidation-sensitive vinyl groups.

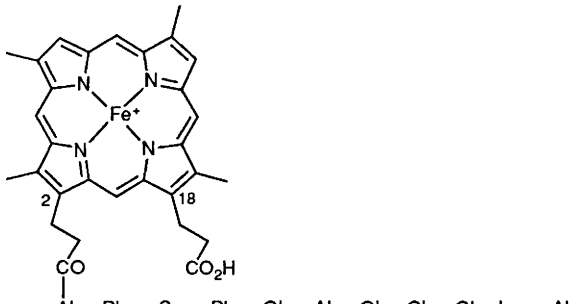

1

Experimental

Materials and Instrumentation.—Compounds accessible from commercial sources were of the highest purity available and used as received. Dimethylformamide (dmf) was purified by treatment with barium oxide and distillation from calcium hydride under reduced pressure. The synthesis of the protected undecapeptide $PhCH_2OCO$-Ala-Phe-Ser-Phe-Glu(OBu^t)-Ala-Gln-Gly-Gly-Leu-Ala-OBu^t is reported elsewhere.[13] Deuterohaemin was prepared from haemin according to a known procedure.[14] The *para*-substituted phenyl methyl sulphides and the corresponding sulphoxides[15,16] were prepared according to literature methods. The concentration of hydrogen peroxide was determined spectrophotometrically.[17] Horseradish peroxidase (mostly isozyme C) was purchased from Sigma as a lyophilized powder (type VI, RZ, Reinheitszahl, A_{403}/A_{275} = 3.2 at pH 7.0). The concentration of enzyme solutions was determined optically using ε_{403} = 102 dm^3 mmol^{-1} cm^{-1}.

Optical absorption spectra were recorded with a HP 8452A

* *Present address:* Dipartimento di Chimica Generale, Universitá di Pavia, Via Taramelli 12, 27100, Pavia, Italy.

diode-array spectrophotometer, mass spectra with a VG 7070 EQ spectrometer, and circular dichroism spectra on a JASCO J-500 C dichrograph.

Removal of N-*Benzyloxycarbonyl Group from the Protected Undecapeptide.*—The peptide $PhCH_2OCO$-Ala-Phe-Ser-Phe-Glu(OBu^t)-Ala-Gln-Gly-Gly-Leu-Ala-OBu^t (1.2 mmol) was dissolved in 80% acetic acid (30 cm^3). Palladium-charcoal (10% palladium content) (0.5 g) was added and the mixture was hydrogenated at atmospheric pressure under stirring, until carbon dioxide evolution ceased. The catalyst was removed by filtration and the filtrate was evaporated to dryness under vacuum. The residue was triturated with diethyl ether, filtered, washed several times with diethyl ether, and dried under vacuum over potassium hydroxide.

Preparation of Deuterohaemin–Undecapeptide **1**.—Deuterohaemin chloride (1 mmol) was dissolved in anhydrous dmf (20 cm^3). Under stirring at 0 °C were added 1-hydroxybenzotriazole (3 mmol) and, after 0.5 h, dicyclohexylcarbodiimide (1 mmol); the mixture was allowed to stir at 0 °C for an additional 1 h. Then the protected undecapeptide (1 mmol) and triethylamine (2 mmol) were added and the mixture was allowed to react at 0 °C for 4 h, followed by 20 h at room temperature. The precipitate of dicyclohexylurea was filtered off and the product was precipitated by addition of diethyl ether (500 cm^3). The crude product was chromatographed on a silica gel column (4 × 30 cm) by eluting with butanol–acetic acid–water (4:1:1 v/v/v). The eluted fractions consisted of unreacted deuterohaemin and peptide, while the deuterohaemin-protected undecapeptide product adhered to the top of the column. It was extracted from the gel by treatment with glacial acetic acid several times, and recovered by concentration of the acetic acid solution to a small volume under vacuum and precipitation with diethyl ether (yield 30%). Cleavage of the *tert*-butyl ester protecting groups was performed by treating the porphyrin complex (50 mg) with trifluoroacetic acid at 0 °C for 2 h, followed by evaporation to dryness under vacuum. The residue was treated with diethyl ether and collected by filtration. Analysis by TLC showed the absence of unreacted deuterohaemin.

Ligand Binding.—The equilibrium constants for ligand–adduct formation by compound **1** were determined by spectrophotometric titrations at 23 °C. The data were analysed assuming simple equilibria of the type (1). The equilibrium

$$M + L \rightleftharpoons ML \quad (1)$$

constant can be expressed by equation (2) where [M], [ML]

$$K = [ML]/[M][L] = \Delta A/(\Delta A_\infty - \Delta A)[L] \quad (2)$$

and [L] represent the concentration of unbound porphyrin complex, porphyrin adduct and free ligand, respectively, in solution; ΔA is the change of absorbance caused by the addition of the ligand and ΔA_∞ the absorbance change at complete adduct formation. The equilibrium constant can be evaluated from the slope of a plot of $1/\Delta A$ against $1/[L]$ according to the double reciprocal equation (3). Formation of adducts with 1:1

$$1/\Delta A = (1/K\Delta A_\infty)(1/[L]) + 1/\Delta A_\infty \quad (3)$$

stoichiometry can be probed by use of the Hill equation in logarithmic form (4). Thus, a plot of log $[\Delta A/(\Delta A_\infty - \Delta A)]$

$$\log [\Delta A/(\Delta A_\infty - \Delta A)] = n \log [L] + \log K \quad (4)$$

against log [L] should give a straight line with slope $n = 1$ when the 1:1 adduct is formed. The concentration of free ligand in solution was evaluated from equation (5),[18] where $[L]_0$ is the total concentration of added ligand and $[M]_0$ the total concentration of porphyrin complex, bound and unbound. Rectilinear regression lines were obtained by least-squares fittings using a computer program that takes into account the volume changes of the solution following each addition of the titrant.

$$[L] = [L]_0 - [M]_0\Delta A/\Delta A_\infty \quad (5)$$

Kinetic Experiments.—The catalase-like activity of deuterohaemin–undecapeptide and deuterohaemin was followed by monitoring dioxygen production with a Clarke oxygen electrode at 20 °C. The reaction systems contained 2.0×10^{-5} mol dm^{-3} iron(III) porphyrin complex and 2×10^{-3} mol dm^{-3} hydrogen peroxide in 0.01 mol dm^{-3} borate buffer, pH 9.0. The initial rates of dioxygen production were 5.5×10^{-7} mol dm^{-3} s^{-1} for **1** and 1.2×10^{-6} mol dm^{-3} s^{-1} for deuterohaemin. The experiment using **1** as catalyst was repeated in the presence of 6.0×10^{-4} and 2.0×10^{-2} mol dm^{-3} L-tyrosine; the resulting initial rate for dioxygen production decreased to 3.8×10^{-7} and 5.0×10^{-8} mol dm^{-3} s^{-1}, respectively.

The kinetics of the catalytic oxidation of thioanisoles by hydrogen peroxide in the presence of compound **1** was studied in thermostatted cells equipped with a magnetic stirrer at 20 °C. The reactant concentrations in the cell were: 1.29×10^{-4} mol dm^{-3} sulphide, 1.0×10^{-6} mol dm^{-3} deuterohaemin–undecapeptide, 5.0×10^{-5} mol dm^{-3} imidazole and 10^{-4} mol dm^{-3} hydrogen peroxide in 0.01 mol dm^{-3} borate buffer, pH 9.0. Reactions were initiated by the addition of hydrogen peroxide and followed spectrophotometrically by the decrease in absorption of the reacting sulphides or, when it was more convenient, by the increase in absorption at the appropriate wavelengths due to the formation of sulphoxides. Initial rates were calculated by using the difference in molar absorption coefficients ($\Delta\varepsilon$) between the the sulphides and the corresponding sulphoxides. The $\Delta\varepsilon$ values (dm^3 mol^{-1} cm^{-1}) employed, determined in 0.01 mol dm^{-3} borate buffer at pH 9.0, and the monitored wavelengths for the *para* X-substituted thioanisoles were as follows: X = F, 11 800 at 252 nm; Cl, −4550 at 230 nm; OCH_3, 2150 at 254 nm; NO_2, −3230 at 280 nm; H, 7630 at 252 nm; CH_3, 6870 at 254 nm. Negative $\Delta\varepsilon$ values indicate the observation of an increase in absorbance during the conversion of sulphide into sulphoxide. No appreciable destruction of the haemin catalyst, monitored through the intensity of the Soret band, occurred within the time of the measurements. The composition of the oxidation products was checked by performing the reactions on a somewhat larger scale; only sulphide and sulphoxide were present in the mixture, as revealed by TLC analysis [SiO_2, diethyl ether–methanol (95:5 v/v) as eluent].

The kinetics of oxidation of tyrosine by hydrogen peroxide and compound **1** was studied at 20 °C in the same apparatus employed for oxidation of the sulphides. Experiments at fixed tyrosine concentration and variable hydrogen peroxide concentration were carried out as follows. The reaction mixtures contained 1.0×10^{-5} mol dm^{-3} deuterohaemin–undecapeptide, 1.0×10^{-3} mol dm^{-3} L-tyrosine, and (1.0–24.0) × 10^{-3} mol dm^{-3} hydrogen peroxide in 0.01 mol dm^{-3} borate buffer, pH 9.0. The reactions were initiated by the addition of hydrogen peroxide and followed by the increase in the absorption band at 315 nm due to the formation of *o,o'*-dityrosine. Initial rates were calculated using the difference in molar absorption coefficients between dityrosine and tyrosine at 315 nm ($\Delta\varepsilon$ 7300 dm^3 mol^{-1} cm^{-1}). Haemin destruction was negligible within the time used for rate determination, but reached about 10% after 1 min at the highest concentrations of H_2O_2 employed.

The kinetics of oxidation of L- and D-tyrosine at variable substrate concentration was followed for reaction mixtures containing 2.5×10^{-6} mol dm^{-3} deuterohaemin–undecapeptide, 5.0×10^{-3} mol dm^{-3} hydrogen peroxide, and (2.8–50.0) × 10^{-4} mol dm^{-3} tyrosine in 0.01 mol dm^{-3} borate buffer, pH 9.0. The reactions were initiated by the addition of the oxidant and

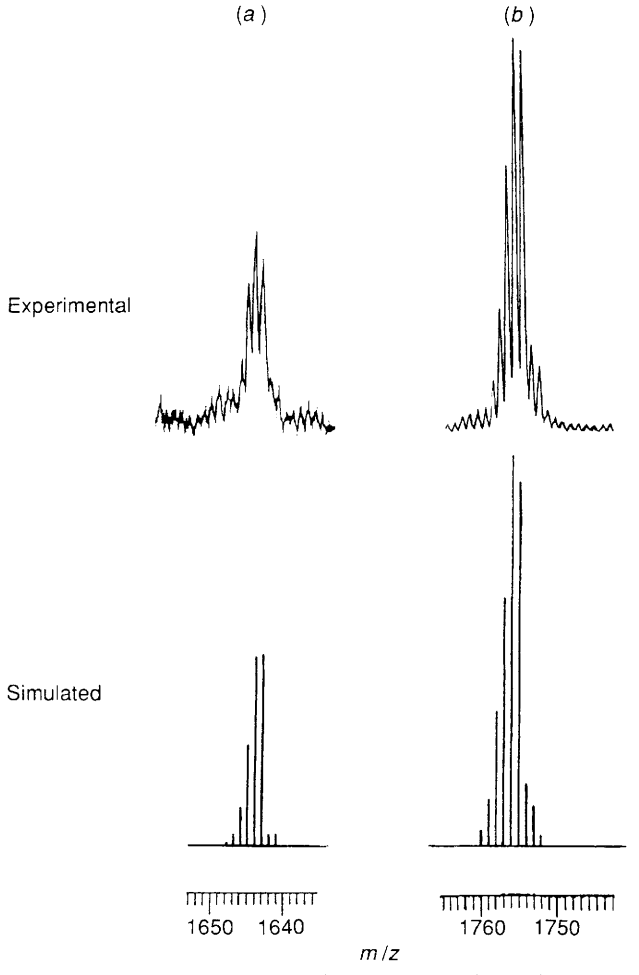

Fig. 1 Experimental and simulated molecular ion clusters in the FAB mass spectra of (*a*) the deuterohaemin–undecapeptide complex and (*b*) its precursor derivative containing two *tert*-butyl ester groups in the peptide chain

followed at 315 nm as described above. The experiments were repeated under the same conditions in the presence of 1.3×10^{-4} mol dm^{-3} imidazole. The pH dependence of the rate of L-tyrosine oxidation was studied in 0.2 mol dm^{-3} phosphate buffer at pH 8.0, 9.0 and 9.5 using 2.5×10^{-6} mol dm^{-3} deuterohaemin–undecapeptide, 5.0×10^{-3} mol dm^{-3} hydrogen peroxide, and 1.1×10^{-3} mol dm^{-3} L-tyrosine. Initial rates were 2.0×10^{-7} mol dm^{-3} s^{-1} at pH 8.0, 5.3×10^{-7} mol dm^{-3} s^{-1} at pH 9.0, and 7.9×10^{-7} mol dm^{-3} s^{-1} at pH 9.5. The kinetics of the horseradish peroxidase-catalysed oxidation of L-and D-tyrosine was studied as follows. The reaction mixtures contained 0.8×10^{-8} mol dm^{-3} enzyme, 9.78×10^{-4} mol dm^{-3} hydrogen peroxide, and $(0.02–5.30) \times 10^{-3}$ mol dm^{-3} tyrosine in 0.05 mol dm^{-3} phosphate buffer, pH 8.2. The reactions were initiated by addition of the oxidant and followed at 315 nm. Initial rates were calculated using $\Delta\varepsilon$ 6700 dm^3 mol^{-1} cm^{-1} for dityrosine formation at pH 8.2.

Results and Discussion

The condensation of the undecapeptide to a propionic acid side chain of deuterohaemin was carried out according to a standard procedure in peptide synthesis, based on the reaction with dicylohexylcarbodiimide and 1-hydroxybenzotriazole, which allows one to work under mild conditions. The resulting deuterohaemin–undecapeptide is a mixture, probably equimolar, of the isomeric compounds containing the peptide chain substituted at positions 2 and 18 of the porphyrin ring. Fig. 1 shows the fast atom bombardment (FAB) mass spectra of the

Table 1 Electronic spectral characteristics of deuterohaemin–undecapeptide derivatives in borate buffer pH 9.0

	UV/VIS, λ_{max}/nm			Relative intensity		
Compound	Soret	β	α	A_{Soret}	A_β	A_α
Fe^{III}	386	488	596	1.00	0.15	0.08
Fe^{II}	410	534		1.00	0.12	
Fe^{II}–CO	400	522	554	1.00	0.09	0.08
Fe^{III}–Him*	390	495	598	1.00	0.14	0.07
Fe^{II}–Him*	408	518	544	1.00	0.11	0.11
Fe^{II}–Him–CO*	406	528	556	1.00	0.09	0.07

* 50 mol equivalents imidazole added to the solution.

deuterohaemin–undecapeptide complex **1** and its precursor derivative containing the two *tert*-butyl ester protecting groups, which gave much more intense peaks, obtained from a 3-nitrobenzyl alcohol matrix. For the latter derivative the molecular ion cluster centred at the expected *m/z* 1755 in the experimental spectrum shows very good correlation with the simulated spectrum, whereas for **1** the spectrum shows contributions from the $[M + 1]^+$ ion (*m/z* 1644). No ions were found at higher *m/z* values, excluding the presence of bis-(peptide) derivatives of deuterohaemin.

The absorption spectrum of compound **1** is very similar to that of deuterohaemin. Upon reduction with sodium dithionite under argon the reduced iron(II) form of the complex is obtained; this reacts with carbon monoxide to produce the Fe^{II}–CO adduct. The spectral data for various derivatives of **1** are collected in Table 1. Of these derivatives the most interesting is certainly the low-spin, six-co-ordinate iron(II)-Him-CO adduct (Him = imidazole), the data for which are identical with those of the carbon monoxide adducts of the imidazole-bound deuterohaemin–histidine [19] and the –serum albumin complexes,[20] confirming that in the latter system a protein imidazole residue is involved in the binding of the haem group. Only very weak induced optical activity is observed in the Soret region for the various derivatives of **1**. Apparently, there is no significant contact between the polar groups on the peptide chain and the metal centre in the porphyrin ring.

Since it is expected that the peptide side chain of compound **1** can fold up to some extent, thereby decreasing the steric accessibility of ligand molecules to the iron centre, it is important to understand the thermodynamics and regiochemistry of ligand binding to the complex. The reaction between simple iron(III) porphyrin complexes [FeP(X)] and nitrogen-containing bases (B) in solution is considered to proceed in two steps [equations (6)–(9)]. In general, when unhindered bases are

$$[FeP(X)] + B \rightleftharpoons [FeP(B)X] \quad (6)$$

$$K_1 = [FeP(B)X]/[FeP(X)][B] \quad (7)$$

$$[FeP(B)X] + B \rightleftharpoons [FePB_2X] \quad (8)$$

$$K_2 = [FePB_2X]/[FeP(B)X][B] \quad (9)$$

employed, formation of the low-spin bis adduct in an apparent single step is observed [equations (10) and (11)]. The stepwise

$$[FeP(X)] + 2\,B \rightleftharpoons [FePB_2X] \quad (10)$$

$$\beta_2 = K_1K_2 = [FePB_2X]/[FeP(X)][B]^2 \quad (11)$$

formation constant K_2 is usually much greater than K_1 so that only the overall formation constant β_2 can be estimated from spectral titrations.[21,22]

Upon addition of a concentrated methanol solution of imidazole to a dilute solution of the deuterohaemin–undecapeptide

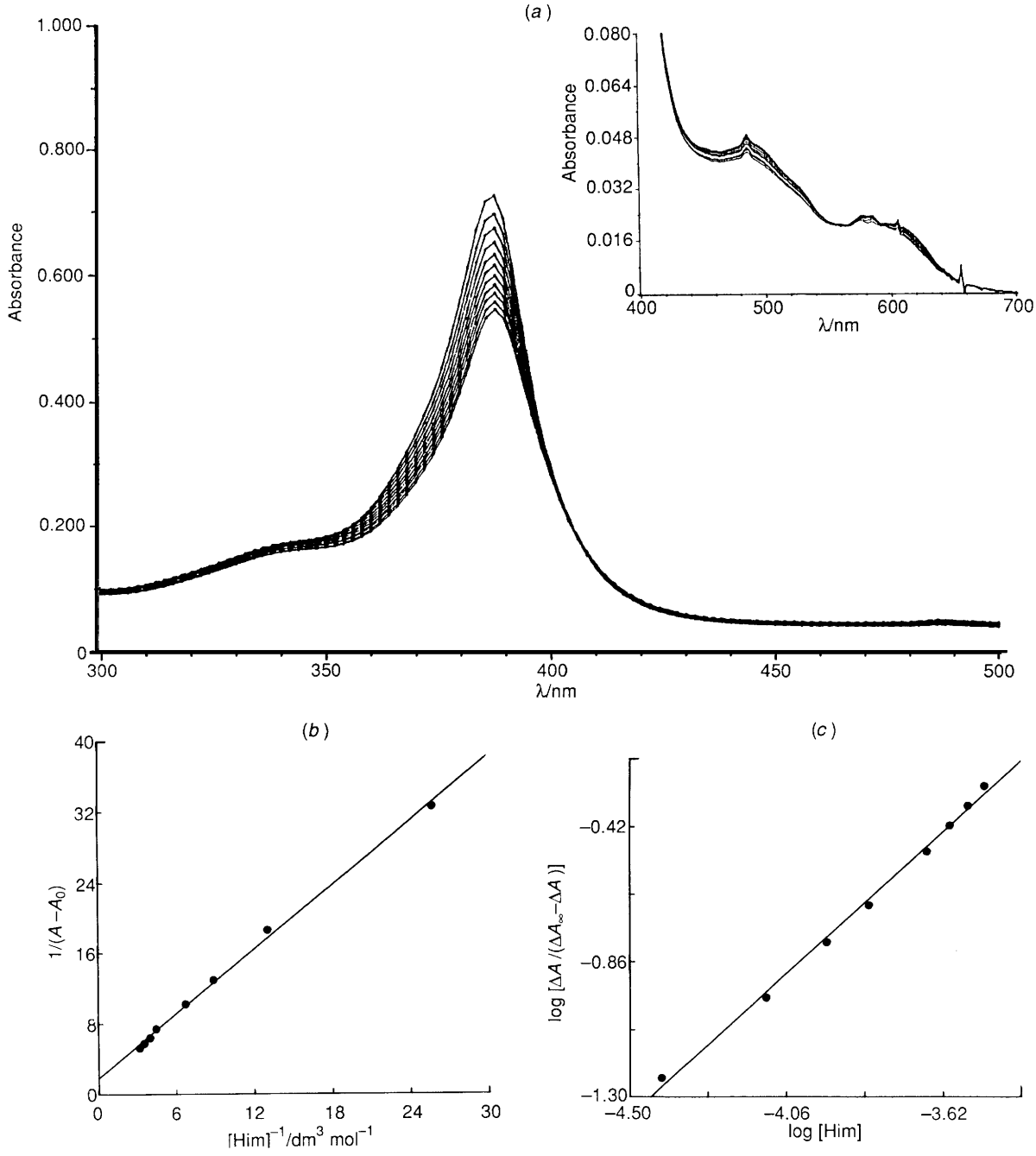

Fig. 2 (*a*) Titration of a 8.0 × 10^{-6} mol dm^{-3} solution of deuterohaemin–undecapeptide in methanol with a 2.4 × 10^{-3} mol dm^{-3} methanolic solution of imidazole (cell path 1.0 cm). The representative spectra show the changes after additions corresponding to [Fe]:[Him] ratios of 1:5, 1:10, 1:15, 1:20, 1:30, 1:35, 1:40, 1:45 and 1:50. The insert shows the changes in the visible region on an expanded scale. (*b*) The corresponding double reciprocal and (*c*) Hill plots at 390 nm

complex the absorption spectrum changes in two steps. With additions of imidazole up to a ratio [Fe]:[Him] of about 1:50 the absorption spectrum undergoes small changes (Fig. 2). The Soret band decreases somewhat in intensity and the position of the maxima near 390, 490 and 590 nm is little affected. This is not surprising since binding of a single imidazole molecule causes little change in the spectrum of the deuterohaemin chromophore, as shown by comparison of the spectra of deuterohaemin (λ_{max} 344, 388, 489 and 587 nm) and the imidazole-bound deuterohaemin–histidine complex [19] (λ_{max} 344, 390, 487 and 585 nm) in methanol solution. The addition of larger amounts of imidazole, up to a [Fe]:[Him] ratio of about 1:1000, produces more marked changes in the absorption spectrum (Fig. 3). The Soret maximum shifts to 400 nm, with an isosbestic point at 395 nm, while the low-energy bands are replaced by a band at about 520 nm, which is characteristic of the low-spin bis(imidazole) adduct.

Analysis of the titration data in the two separate binding steps according to the procedure cutlined in the Experimental section gives the values of K_1 = 1500 dm^3 mol^{-1} (n = 1.05) and K_2 = 220 dm^3 mol^{-1} (n = 0.96). It is therefore clear that binding of an imidazole molecule in the fifth axial position (**2**) produces a folding in the peptide side chain of **1** such that the accessibility of the sixth axial position is sterically reduced in a significant manner.

The presence of a bulky peptide residue covalently bound to the porphyrin ligand has the important effect of enhancing the stability of **1** towards oxidative haemin destruction by oxidizing agents like hydrogen peroxide or *tert*-butyl hydroperoxide, with respect to *e.g.* deuterohaemin or deuterohaemin–histidine, as

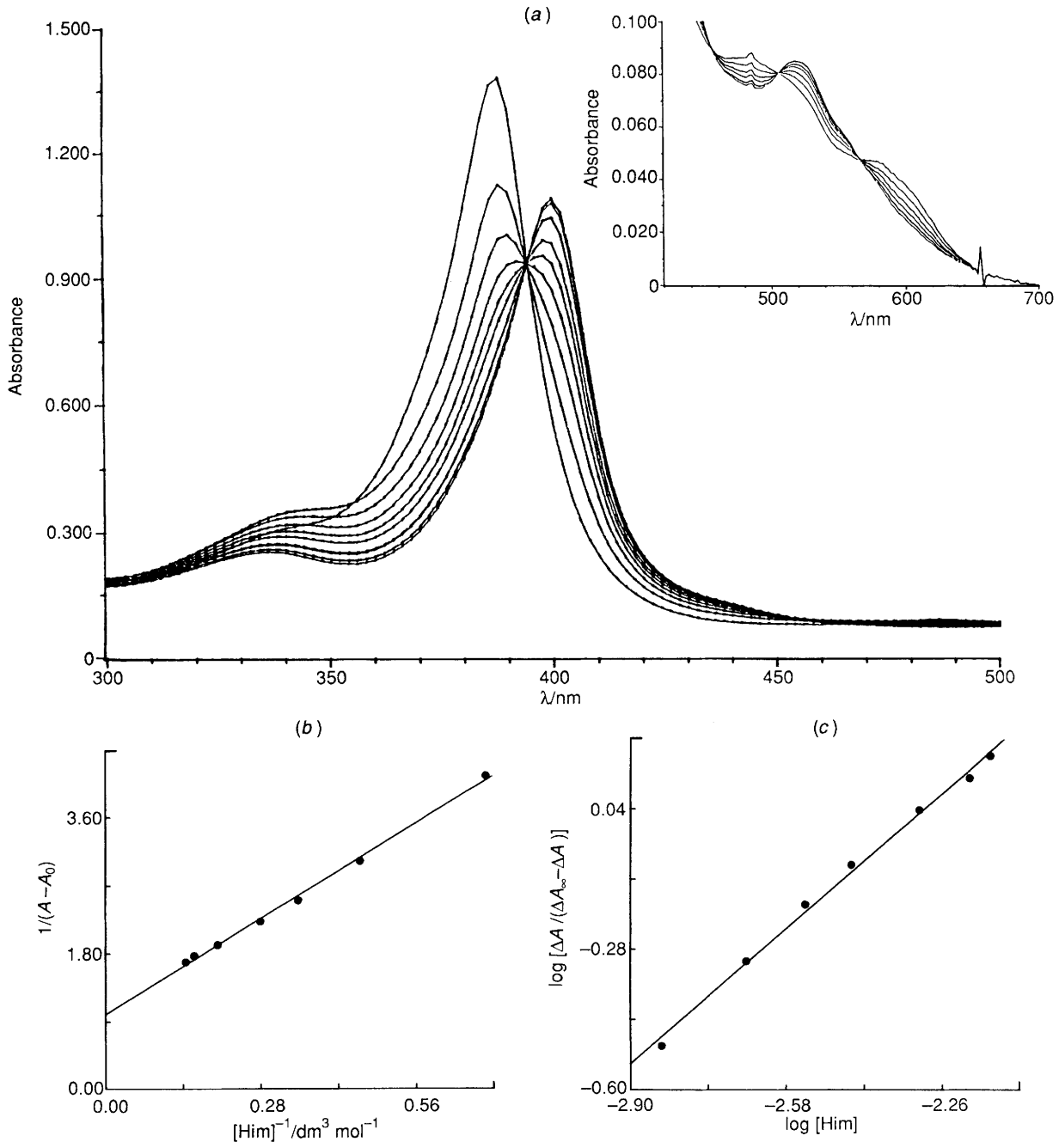

Fig. 3 (*a*) Titration of 7.2×10^{-6} mol dm^{-3} solution of deuterohaemin-undecapeptide in methanol with a 0.1 mol dm^{-3} methanolic solution of imidazole (cell path 2.0 cm). The representative spectra show the changes after additions corresponding to [Fe]:[Him] ratios of 1:100, 1:200, 1:300, 1:400, 1:500, 1:600, 1:700, 1:800 and 1:900. The insert shows the changes in the visible region on an expanded scale. (*b*) The corresponding double reciprocal and (*c*) Hill plots at 402 nm

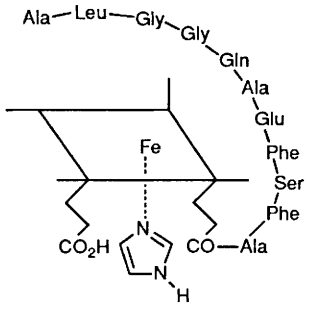

2

shown by comparative experiments. Attempts to observe spectroscopically high-valent iron porphyrin intermediates were unsuccessful. Upon reaction of **1** with stoichiometric amounts of hydrogen peroxide negligible changes in the haemin absorption spectrum occurred. This result depends on the fact that the deuterohaemin–undecapeptide complex is active in the catalytic decomposition of hydrogen peroxide. Increasing the concentration of hydrogen peroxide had only the effect of producing a significant decrease in the Soret absorption as the result of porphyrin degradation. For this reason the catalatic activity was not investigated in detail. Under the same conditions the initial rate of dioxygen production from hydrogen peroxide by **1** was found about one half that exhibited by deuterohaemin. However, the catalatic activity was depressed in the presence of electron-donor substrates, indicating that the catalytic oxidation of these molecules by hydrogen peroxide can effectively compete with decomposition of the oxidant. We choose to investigate here in some detail the

oxidations of substituted aryl alkyl sulphides and tyrosine, which are typical substrates of peroxidase enzymes.

The participation of peroxidases in the biotransformation of organic sulphides may represent important steps in the mammalian detoxification processes of this relevant class of environmental chemicals.[23–25] The sulphides are normally converted into sulphoxides in these reactions, but when the substrate contains acidic α-protons disulphides can be formed as stable by-products of S-dealkylation.[26] The mechanism of the peroxidase oxidation of sulphides is complex and not fully understood.[27] Basically, two limiting mechanisms can be considered: the one-step oxygen-transfer mechanism, where the oxygen atom is transferred concertedly from the intermediate Compound I to the sulphide [equations (12) and (13)]; and the

$$Fe^{3+} + H_2O_2 \longrightarrow (Fe{=}O)^{3+} + H_2O \quad (12)$$

$$(Fe{=}O)^{3+} + R{-}S{-}R' \longrightarrow Fe^{3+} + R{-}SO{-}R' \quad (13)$$

two-step mechanism, where one-electron reduction of Compound I produces a sulphur cation radical and the intermediate Compound II, followed by the reaction that leads to the sulphoxide [equations (12), (14) and (15)]. Here Fe^{3+}, $(Fe{=}O)^{3+}$

$$Fe^{3+} + H_2O_2 \longrightarrow (Fe{=}O)^{3+} + H_2O \quad (12)$$

$$(Fe{=}O)^{3+} + R{-}S{-}R' \longrightarrow (Fe{=}O)^{2+} + R{-}\overset{\bullet+}{S}{-}R' \quad (14)$$

$$(Fe{=}O)^{3+} + R{-}\overset{\bullet+}{S}{-}R' \longrightarrow Fe^{3+} + R{-}SO{-}R' \quad (15)$$

and $(Fe{=}O)^{2+}$ represent the native enzyme, and the peroxidase intermediates I and II, respectively. It is generally thought that direct transfer of the ferryl oxygen atom to the substrate cannot occur in peroxidase reactions,[28] therefore reaction (15) would involve the attack of a hydroxyl radical released from Compound II on the sulphur cation.[27] However, the direct transfer of oxygen from hydroperoxide to the sulphur atom observed during the oxidation of thioanisoles by horseradish peroxidase remains to be explained,[29] and chloroperoxidase is believed to catalyse the oxidation of organic sulphides by hydrogen peroxide through the one-step oxygen-transfer mechanism.[15]

Kinetic studies can provide information on the type of mechanism involved. For instance, in the electrophilic oxidation of thioanisoles **3** the reaction rates are expected to increase with the electron-donating properties of the X substituent. However, in a Hammett plot[30] the logarithm of the reaction rates correlates with the σ_p parameter according to equation (13) and with the σ^+ parameter according to equation (14). Previously, the relative reactivities of *para*-substituted thioanisoles in the sulphoxidation reaction (16) were found to correlate with the Hammett σ^+ values when lactoperoxidase[26] or synthetic haemins[31,32] were used as catalysts, and with σ_p in the chloroperoxidase-dependent reaction.[15] Correlations for σ_p and σ^+ were both very poor in the sulphoxidation mediated by horseradish peroxidase,[15] reflecting the probable existence of competitive mechanisms.

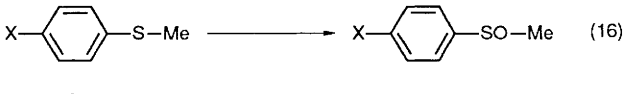

(16)

3 **4**

The deuterohaemin–undecapeptide complex **1** catalyses the oxidation of thioanisoles **3** by hydrogen peroxide. Imidazole accelerates the reaction, but it is not absolutely necessary for it, at least in the basic medium employed here. The rather low solubility of the sulphides prevent study of the catalytic oxidation over a concentration range, however by carrying out

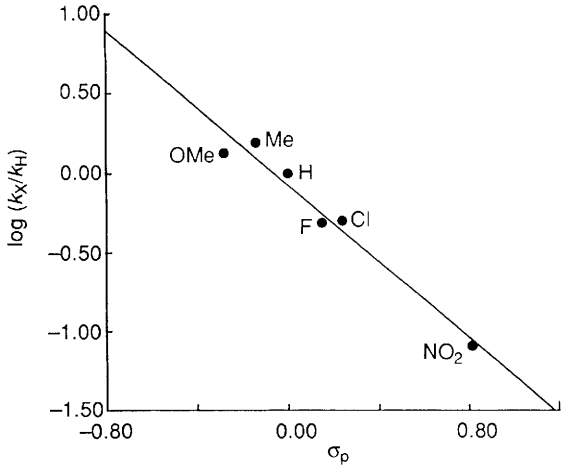

Fig. 4 Linear free-energy plot of initial rates for the formation of *para*-substituted thioanisole sulphoxides catalysed by deuterohaemin–undecapeptide in 0.01 mol dm^{-3} borate buffer, pH 9.0. The logarithms of the rates, in mmol dm^{-3} s^{-1}, determined as described in the Experimental section are plotted. For reference compound with X = H, log k_H = −7.6

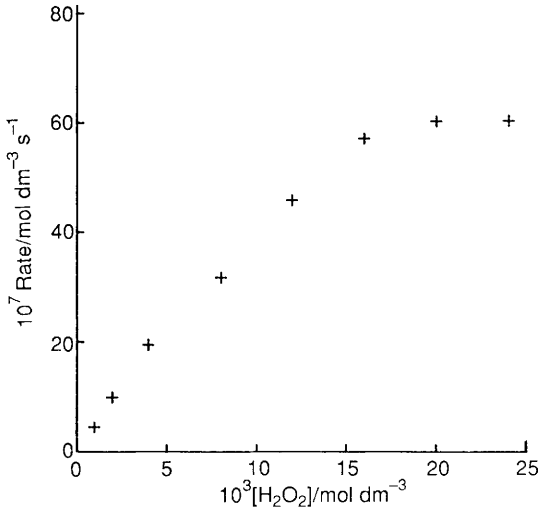

Fig. 5 Dependence on hydrogen peroxide concentration of the initial rates of dityrosine formation in the oxidation catalysed by deuterohaemin–undecapeptide (borate buffer, pH 9.0)

reactions under identical conditions the relative initial rates of oxidation can be taken as an index of reactivity of the substrates. The competitive catalytic activity produces only a reduction in the effective hydrogen peroxide concentration available for oxidation. The reactivity of *para*-substituted thioanisoles increases with the electron-donating properties of the substituents and a good correlation is found between the reaction rates and the Hammett σ_p values ($\rho = -1.21$, $r = 0.980$), Fig. 4, while the correlation for σ^+ is poorer ($\rho = -0.36$, $r = 0.880$). It is worth noting that the reaction constant value found for the chloroperoxidase-catalysed reaction ($\rho = -1.40$)[15] is similar to that found here using **1**. Although some competition cannot be excluded, these results suggest that a concerted insertion of the oxygen by the iron active species into the sulphide represents the main route for the oxidation. Binding experiments exclude direct co-ordination of the sulphides to the iron centre to any significant extent, but these substrates may interact with the peptide chain of **1**. Possibly, the presence of phenylalanine residues in the undecapeptide assists in the binding and appropriate juxtaposing of the sulphide with respect to the haem iron to allow the oxygen-transfer reaction. A similar situation apparently characterizes the binding of substituted thioanisoles to chloroperoxidase,[33] while haem accessibility to

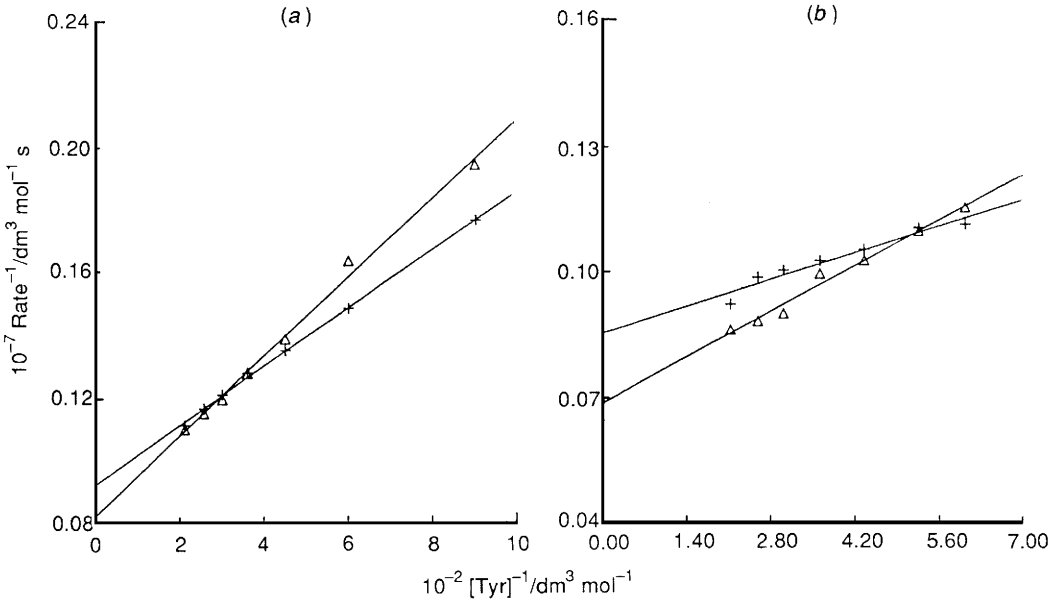

Fig. 6 Plots of 1/rate *vs.* 1/[substrate] (Lineweaver–Burk plots) for the oxidation of tyrosine catalysed by compound **1**: (*a*) oxidation of L- (+) and D-tyrosine (Δ) in borate buffer, pH 9.0. (*b*) Oxidation of L- and D-tyrosine under the same conditions but in the presence of imidazole

the substrates is known to be limited in normal peroxidases so that the reactions occur at the haem edge.[28]

The peroxidase-catalysed oxidation of tyrosine has biological relevance because this amino acid and its derivatives are among the most important electron donors in mammalian systems. The main product of the reaction, at least in the early stages, is the dimer α,α′-diamino-6,6′-dihydroxy-1,1′-biphenyl-3,3′-dipropanoic acid (*o*,*o*′-dityrosine).[34] The deuterohaemin–undecapeptide complex was found to catalyse the same oxidative coupling reaction of tyrosine by hydrogen peroxide as did the peroxidases. In order to investigate the reaction in some detail we had to consider that the peroxidase activity of compound **1** is in competition with the catalytic decomposition of hydrogen peroxide. However, by increasing the H_2O_2 concentration we may expect to reach a saturation condition above which the rate of tyrosine oxidation does not increase further on increasing the hydrogen peroxide concentration. In Fig. 5 it is shown that the initial rate of tyrosine oxidation catalysed by **1** (ratio [L-Tyr]:[**1**] = 100:1) actually reaches a plateau on increasing the oxidant concentration (at $[H_2O_2]$:[L-Tyr] = 20:1). The plateau region is reached at lower hydrogen peroxide concentration as the tyrosine concentration is increased, because the catalatic activity is progressively depressed, and it requires higher $[H_2O_2]$ as the tyrosine concentration is decreased. We thus investigated the rate of tyrosine oxidation over a substrate concentration range under saturating H_2O_2 conditions, but excluded the range below [Tyr]:[**1**] = 100:1 because the high concentrations of hydrogen peroxide required produced significant haemin destruction during the experiments. The reaction was investigated with both the L and D isomers of the substrate in the absence and presence of imidazole as a donor ligand for the iron, and the results were compared with those for the horseradish peroxidase-catalysed oxidation of L- and D-tyrosine. The initial rates of the reactions catalysed by **1** in all cases approached limiting values at high substrate concentrations (Fig. 6). This suggests that the kinetic scheme can be described by the Michaelis–Menten relationship, [35] which characterizes the peroxidase-catalysed reaction and many other enzymatic reactions [36] [equation (17)]. In this

$$\underset{\mathbf{5}}{Fe_{ox}} + \text{phenol} \underset{k_{-1}}{\overset{k_1}{\rightleftharpoons}} \underset{\mathbf{6}}{Fe_{ox}(\text{phenol})} \xrightarrow{k_2} Fe^{3+} + \text{product} \qquad (17)$$

scheme the substrate (phenol) binds reversibly to the active iron oxo species **5**, forming an oxoiron–substrate intermediate **6** which irreversibly decomposes to the product and Fe^{3+} in the rate-determining step. In the peroxidase-catalysed reactions the rate-determining step is usually the reaction between the electron donor and Compound II.[37] If a similar behaviour is assumed here for **1**, the Fe_{ox} species **5** can be identified as an $(Fe{=}O)^{2+}$ species. The kinetic parameters V_{max} and K_m, where $V_{max} = k_2[Fe]_{total}$ directly measures the rate-limiting decay of **6** and $K_m = (k_{-1} + k_2)/k_1$, in the limit that $k_{-1} \gg k_2$, gives a measure of the dissociation constant of **6**, can be estimated from the double reciprocal plots (Lineweaver–Burk plots)[38] shown in Fig. 6 according to equation (18).

$$\frac{1}{\text{rate}} = \frac{K_m}{V_{max}} \cdot \frac{1}{[\text{phenol}]} + \frac{1}{V_{max}} \qquad (18)$$

The kinetic results are collected in Table 2 in terms of k_{cat}, the maximum activity of the catalyst under the specified conditions, expressed as mol of dityrosine produced per mol of catalyst per second (i.e. turnover per second) and K_m. Under substrate-saturating conditions the deuterohaemin–undecapeptide complex exhibits a slight preference for the oxidation of D- with respect to L-tyrosine. However, the affinity of the D isomer for the catalyst is lower than that of the L isomer. This implies that at low (*i.e.* lower than K_m) substrate concentration, where the activity of the catalyst can be expressed by k_{cat}/K_m,[36] the stereoselectivity of the reaction is reversed. The presence of imidazole slightly increases k_{cat} and decreases K_m for both L- and D-tyrosine, so that the preference for L-tyrosine

Table 2 Kinetic parameters for the catalytic oxidation of L- and D-tyrosine by hydrogen peroxide at 20 °C[a]

Catalyst	Substrate	k_{cat}/s^{-1}	K_m/mmol dm^{-3}	$k_{cat}K_m^{-1}$/dm^3 mol^{-1} s^{-1}
1	L-Tyr	0.43	1.05	0.41
1	D-Tyr	0.47	1.48	0.26
1 + Him	L-Tyr	0.46	0.51	0.90
1 + Him	D-Tyr	0.56	1.15	0.49
hrp[b]	L-Tyr	3.2	3.25	0.98
hrp	D-Tyr	12.0	2.92	4.11

[a] Conditions as indicated in the Experimental section. [b] hrp = Horseradish peroxidase.

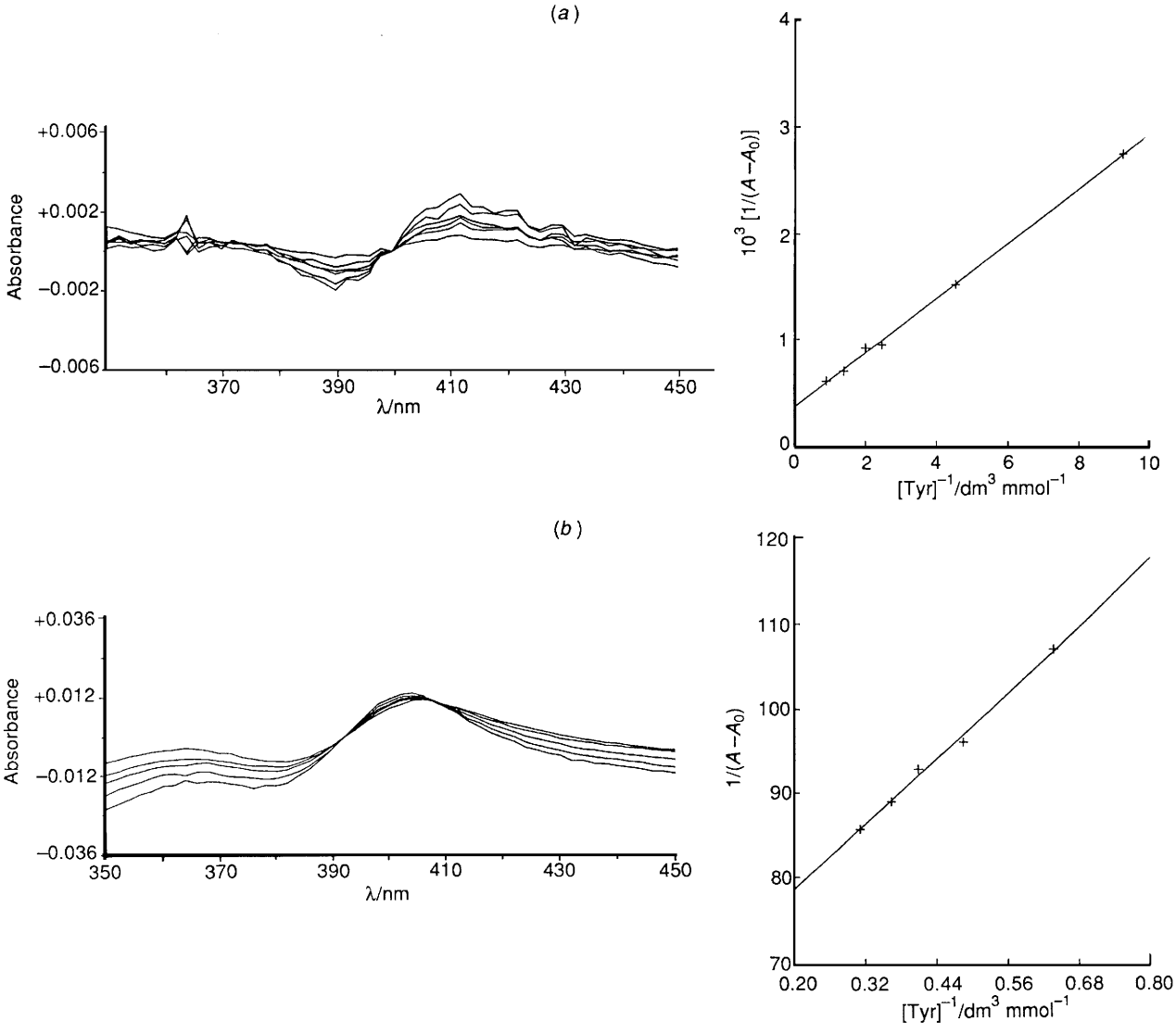

Fig. 7 Difference spectra obtained on titration of deuterohaemin–undecapeptide with tyrosine in borate buffer, pH 9.0 (cell path 1.0 cm). (*a*) Titration with L-Tyr; 2.8 × 10^{-6} mol dm^{-3} deuterohaemin–undecapeptide; the curves correspond to [Fe]:[L-Tyr] ratios of 1:40, 1:80, 1:160, 1:200, 1:300 and 1:500. The corresponding double reciprocal plot is also shown. (*b*) Titration with D-Tyr; deuterohaemin–undecapeptide 2.8 × 10^{-5} mol dm^{-3}; the curves correspond to [Fe]:[D-Tyr] ratios of 1:34, 1:60, 1:88, 1:140 and 1:210. The corresponding double reciprocal plot is also shown

oxidation at low substrate concentration becomes more marked.

The difference in K_m values for the two tyrosine isomers is not surprising if we take into account that the interaction of the substrates with the catalyst, to form the adducts **6**, is likely to involve the peptide chain of **1** containing several chiral amino acid residues. This is confirmed by studies of the binding of L- and D-Tyr to the resting form of deuterohaemin–undecapeptide. Addition of the amino acids to **1** (up to a ratio of [Tyr]:[**1**] = 4000:1) in borate buffer, pH 9.0, produces extremely small changes in the absorption spectrum of the complex; these are shown as difference spectra in Fig. 7. The extent of these changes seems to exclude direct co-ordination of tyrosine to the iron(III) centre and can be better explained assuming an interaction in the vicinity of the haem. In any case both the shape of the curves and the binding constant derived from the titration data (K = 1300 dm^3 mol^{-1}, n = 1.01, for L-Tyr; 980 dm^3 mol^{-1}, n = 1.06, for D-Tyr) show that the behaviour of the two tyrosine isomers is different, so that an interaction of the amino acid with the peptide backbone of **1** seems necessarily involved. The binding data also confirm the higher affinity of L- with respect to D-Tyr found in the kinetic experiments.

As for the form of the substrate, phenol or phenolate, which undergoes the peroxidatic reaction, probably the anionic form of tyrosine is the reactive form since the rate of oxidation was found to increase with pH. A similar behaviour was observed in the oxidation of phenol by hydrogen peroxide catalysed by deuterohaemin.[39]

Table 2 reports some kinetic data obtained for the oxidation of L- and D-tyrosine by horseradish peroxidase. Although the enzymatic data are not directly comparable with those of compound **1**, because they were necessarily obtained in different conditions, it is clear that for the oxidation of L- and D-tyrosine the difference in K_m values is now less important. The efficiency of the enzymatic oxidation is much higher for both the tyrosine isomers but the difference in k_{cat} for L- and D-tyrosine is so large that the stereoselectivity is practically unchanged througout the range of substrate concentrations. As is discussed in more detail elsewhere,[40] here the difference in reactivity between L- and D-tyrosine depends on the specific mode of binding and degree of immobilization of the substrates in the active site of the enzyme, so that the more tightly bound isomer is also the more reactive, probably because electron transfer from the phenol nucleus to the haem during the catalytic cycle is facilitated. This aspect is crucial for the activity of enzymatic systems, but it is obviously the most difficult to mimic in model systems.

Acknowledgements

The authors thank the 'Progetto Finalizzato – Chimica Fine' of the Italian Consiglio Nationale delle Ricerche for financial support, P. Russo for the FAB mass spectral measurements, S. Poli for the experiments on horseradish peroxidase and S. Colonna for samples of sulphides and sulphoxides. We also thank one of the referees for drawing our attention to the potential catalatic activity of deuterohaemin complex.

References

1 T. Higuchi, T. Mori, S. Uzu and M. Hirobe, *Stud. Org. Chem.*, 1988, **33**, 455.
2 T. Sasaki and E. T. Kaiser, *J. Am. Chem. Soc.*, 1989, **111**, 380.
3 F. Niedercorn, H. Ledon and I. Tkatchenko, *New. J. Chem.*, 1988, **12**, 897.
4 T. Mashino, S. Nakamura and M. Hirobe, *Tetrahedron Lett.*, 1990, **31**, 3163.
5 P. A. Adams and R. D. Goold, *J. Chem. Soc., Chem. Commun.*, 1990, 97.
6 D. A. Baldwin, H. M. Marques and J. M. Pratt, *J. Inorg. Biochem.*, 1987, **30**, 203.
7 P. A. Adams, M. P. Byfield, R. C. de L. Milton and J. M. Pratt, *J. Inorg. Biochem.*, 1988, **34**, 167.
8 P. A. Adams and C. Adams, *J. Inorg. Biochem.*, 1988, **34**, 177.
9 K. Ohkubo, H. Ishida and T. Sagawa, *J. Mol. Catal.*, 1989, **53**, L5; M. Barteri, P. Jones and O. Mantovani, *J. Chem. Soc., Dalton Trans.*, 1986, 333.
10 D. Mansuy, P. Battioni and J.-P. Battioni, *Eur. J. Biochem.*, 1989, **184**, 267.
11 D. Mansuy, *Pure Appl. Chem.*, 1990, **62**, 741.
12 T. Okamoto, K. Sasaki and M. Tachibana, *Bull. Inst. Chem. Res., Kyoto Univ.*, 1989, **67**, 169.
13 F. Chillemi, S. Cappelletti, P. Francescato and A. Chersi, *Int. J. Peptide Protein Res.*, 1990, **35**, 271.
14 J. H. Fuhrhop and K. M. Smith, *Laboratory Methods in Porphyrin and Metalloporphyrin Research*, Elsevier, Amsterdam, 1975, p. 17.
15 S. Kobayashi, M. Nakano, T. Kimura and A. P. Schaap, *Biochemistry*, 1987, **26**, 5019; H. L. Holland and I. M. Carter, *Can. J. Chem.*, 1982, **60**, 2420; H. L. Holland, *Chem. Rev.*, 1988, **88**, 473.
16 S. Colonna, N. Gaggero, A. Manfredi, L. Casella, M. Gullotti, G. Carrea and P. Pasta, *Biochemistry*, 1990, **29**, 10465.
17 D. P. Nelson and L. A. Kiesow, *Anal. Biochem.*, 1972, **39**, 474.
18 K. L. Brown, *Inorg. Chim. Acta*, 1979, **37**, L513.
19 M. Momenteau, M. Rougee and B. Loock, *Eur. J. Biochem.*, 1976, **71**, 63; M. Okuyama, T. Murakami, T. Nozawa and M. Hatano, *Chem. Lett.*, 1982, 111.
20 L. Casella, M. Gullotti, S. Poli and L. De Gioia, sumitted for publication.
21 F. A. Walker, M. W. Lo and M. T. Ree, *J. Am. Chem. Soc.*, 1979, **98**, 5552.
22 T. Yoshimura and T. Ozaki, *Bull. Chem. Soc. Jpn.*, 1979, **52**, 2268.
23 R. A. Neal and D. Halpert, *Annu. Rev. Pharmacol. Toxicol.*, 1982, **22**, 321.
24 D. R. Doerge and M. D. Corbett, *Mol. Pharmacol.*, 1984, **26**, 348.
25 D. R. Doerge, *Arch. Biochem. Biophys.*, 1986, **244**, 678.
26 D. R. Doerge, G. L. Pitz and D. P. Root, *Biochem. Pharmacol.*, 1987, **36**, 972.
27 U. Pérez and H. B. Dunford, *Biochemistry*, 1990, **29**, 2757.
28 P. R. Ortiz de Montellano, *Acc. Chem. Res.*, 1987, **20**, 289.
29 S. Kobayashi, N. Minoru, T. Goto, T. Kimura and A. P. Schaap, *Biochem. Biophys. Res. Commun.*, 1986, **135**, 166.
30 J. March, *Advanced Organic Chemistry*, 3rd edn., McGraw-Hill, New York, 1985, ch. 9.
31 S. Oae, Y. Watanabe and K. Fujimori, *Tetrahedron Lett.*, 1982, **23**, 1189.
32 T. Mashino, S. Nakamura and M. Hirobe, *Tetrahedron Lett.*, 1990, **31**, 3163.
33 L. Casella, M. Gullotti, R. Ghezzi, S. Poli, T. Beringhelli, G. Carrea and S. Colonna, unpublished work.
34 G. S. Bayse, A. W. Michaels and M. Morrison, *Biochim. Biophys. Acta*, 1972, **284**, 34.
35 L. Michaelis and M. L. Menten, *Biochem. Z.*, 1913, **49**, 333.
36 See, for instance, A. Fersht, *Enzyme Structure and Mechanism*, 2nd edn., Freeman, New York, 1985.
37 H. B. Dunford and J. S. Stillman, *Coord. Chem. Rev.*, 1976, **19**, 187.
38 H. Lineweaver and D. Burk, *J. Am. Chem. Soc.*, 1934, **56**, 658.
39 P. Jones, D. Mantle and I. Wilson, *J. Inorg. Biochem.*, 1982, **17**, 293.
40 L. Casella, M. Gullotti, S. Poli, M. Bonfà, R. P. Ferrari and A. Marchesini, *Biochem. J.*, in the press.

Received 14*th January* 1991; *Paper* 1/00170A